23rd ABCM International Congress of Mechanical Engineering
December 6-11, 2015, Rio de Janeiro, RJ, Brazil

ERYTHRITOL MELT FRACTION CORRELATION FOR TALL ENCLOSURE PCM BASED HEAT SINKS

João Fidelio Raymundo Júnior
Rejane De Césaro Oliveski
Universidade do Vale do Rio dos Sinos – UNISINOS – Av. Unisinos 950, São Leopoldo, RS 93022-000, Brazil
jraymundojunior@gmail.com; decesaroo@gmail.com

Abstract. *Many areas of engineering use thermal energy storage to optimize performance, such as the case of petrochemical and food industries and many liquid heating/cooling systems. Thermal energy storage systems can be used as either a heat source or heat sink. In the applications with intermittent energy generation, such as wasted heat recovery and electronic devices cooling systems, an appropriate thermal storage/release system is essential. The thermal storage/release technology based on the use of phase change materials (PCMs) has raised huge practical interest, due to its great heat accumulation capacity. Phase change phenomena occurring during PCM melting need to be carefully controlled and understood. Such optimization requires extensive thermal and dynamic knowledge of the materials within the tanks. Some studies have been carried out to investigate the thermal and hydrodynamic characteristics of the phase change phenomena involved in these systems. Most of these are experimental and only a few use a numerical approach, and most of them use low melting point PCMs. This study focuses studying and analyzing these phase change characteristics in a tall enclosure heat sink with plate fins through CFD (computational fluid dynamics). The PCM utilized is Erythritol. It has a higher melting point compared to most other PCMs, which has drawn interest in the recent years. The simulations were carried out through CFD, using the FLUENT (v14) software, in a 3D domain, which consists of three materials, the PCM, aluminum and air. The mesh used is structured, hexaedrical and refined near the walls and the PCM-air interface. The mathematical model is made of the mass, momentum and energy conservation equations and was validated using results available in the literature. The walls are impermeable and a non-slip condition is adopted. They also have a constant temperature, except for the bottom wall, which is adiabatic. Three temperature differences (10, 15 and 20 °C) between the PCM initial temperature and domain walls are analyzed. Geometric parameters are also taken into account, such as enclosure height (10, 20 and 30 cm) and distance between the fins (2, 3 and 4 mm). Over 25 different cases were simulated. Among other analysis conducted based on these simulations, a correlation is proposed. It relates many non-dimensional numbers such as Rayleigh number and Fourier number to the PCM's melt fraction, which links the liquid and solid PCM volumes.*

Keywords: *PCM, Correlation, Thermal Storage, Erythritol, CFD*

1. INTRODUCTION

Many areas of engineering use thermal energy storage to optimize performance, such as the case of petrochemical and food industries and many liquid heating/cooling systems. Thermal energy storage systems can be used as either a heat source or heat sink. In the applications with intermittent energy generation, such as wasted heat recovery, ground heat thermal and solar thermal systems, an appropriate thermal storage/release system is essential. The thermal storage/release technology based on the use of phase change materials (PCMs), which possess a great capacity of accumulating energy for consideration as heat storage media, has raised an important practical interest (Barba and Spiga, 2003). Indeed, the improved storage density and the constant temperature release of energy allow a more compact heat exchanger design and simplify system management. Phase change phenomena occurring during PCM melting and PCM solidification need to be carefully controlled. This effective optimization requires an extensive knowledge of the thermal and dynamic behavior of the fluid within the tanks.

Shatikian *et al.* (2005) conducted a numerical exploration for the melting process of PCM in a rectangular unit with internal fins open to air at its top. The melting process occurs at low temperature (23-25 ºC) with RT25 paraffin. A parametric investigation is performed in a small system and the temperature of the base varies from 6ºC to 24 ºC above the mean melting temperature of the PCM. The results show how the transient process depends on the thermal and geometrical parameters of the system. Dimensional analysis of the results is performed and presented as the Nusselt numbers and melt fractions vs. the Fourier and Stefan numbers. (Rathod and Benerjee, 2013).

Most organic PCMs have extremely low thermal conductivity for this type of use, making it difficult completely utilize its heat storage capacity. The heat transfer rate is usually enhanced by the incorporation of highly thermal

conductive materials, often called thermal conductivity enhancers (TCE) into the PCM. These TCE are distributed in the PCM in the form of metal matrixes, fins or dispersed particles (Saha and Dutta, 2010).

Paraffin has drawn considerable attention in the latest years, due to its wide range of melting temperatures, depending on the specific material. Most studies conducted in the recent years utilized paraffin as PCM, such as Shmueli *et al.* (2010) and Assis *et al.* (2007) with RT27 and Al-Abidi *et al.* with RT82. In these studies, the maximum melting temperature is 82 °C, while the properties of paraffin have been studied to up to 90 °C. In the present study, Erythritol is used as PCM, due to its higher melting point compared to paraffin (118 °C), allowing its use in applications which require higher operation temperatures.

Saha and Dutta (2010) conducted a numerical study to stablish Nusselt number correlations for different types of PCM based heat sinks. Shallow, rectangular and tall enclosures were studied. It was concluded that a single correlation for Nusselt number with Rayleigh number was not appropriate for all aspect ratios. However, the study assumed a constant heat flux from the bottom of the domain for all the three cases. The authors presented two Nusselt correlations with different characteristic lengths for different types of aspect ratios.

Various parameters influence the melting process, which determine the performance of the heat sink. So, it is important to establish heat transfer and melt fraction correlations based on relevant non-dimensional numbers, to allow easier development of these heat sinks. The aim of the present work is, through a numerical analysis, establish a correlation between the PCM melt fraction and others non-dimensional numbers, to be used on design of heat sinks. The model utilized considers a different approach from other studies in the literature, considering a constant temperature on the side walls, instead that of a heat flux.

2. NUMERICAL STUDY

The physical problem, the numerical model and the solution method are presented in this section. The validation of the implemented numerical model is presented at the end of this item.

2.1 Physical Model

The thermal energy storage (TES) consists of a system presented in Fig. 1(a). This system is a square channel with inner fins and filled with PCM inside the cavities. The heat transfer fluid (HTF), water, flows through the external vertical channels and exchange heat with the PCM through the aluminum walls.

The system consists of multiple cavities containing Erythritol as PCM, as seen in Figs. 1 (a-b).In this case, there is symmetry in the half of the thickness ($2e$) of the inner fins, as well as at positions that separate the system into four quadrants. In addition, the HTF temperature is kept constant and the metal wall that separates the PCM is thin. With these conditions, we can consider that the temperature of the all vertical walls, between water and PCM, are constant. Thus, it can be considered the three symmetry regions, shown in Fig. 1(b) through the dashed lines. The three-dimensional view of the latter region can be seen in Fig. 1 (c), which was used as computational domain of the 3D cases (Fig. 1(c)). This calculation domain has dimensions H=200 mm, W=2 mm, B=5 mm and e=0.5 mm. If the TES not have internal fins, it can be considered that there is no influence of the back and front walls, in a parallel plane to these, in the cavity middle. In this case, it can be considered the TES as a 2D problem, as shown in Fig. 1 (d).

To take account the volume expansion during solid-liquid phase change due to the large difference in solid and liquid density of PCM that exists in reality, the cavities are filled with only 180 mm of PCM and the rest is filled with air only.

Physical properties of the PCM are needed to conduct the experiment, including melting point, latent heat capacity (L), density, specific heat and viscosity. Despite an extensive research, physical properties were found in only three references (Agyenim *et al.* (2010), Hesaraki (2010), and Sillick and Gregson (2012)). In the work of Agyenim *et al.* (2010) no viscosity values were presented. These values were obtained in the numerical work of Hesaraki (2010). However, the last author used linear variation with temperature for all properties. Sillick and Gregson (2012) presented experimental results of erythritol viscosity, which shows that the variation is logarithmic with the temperature. The viscosity values used were the ones presented by Silik and Gregson (2012). The other properties are those used by Agyenim *et al.* (2010) and Hesaraki (2010). Table 1 shows all the properties values used in this work.

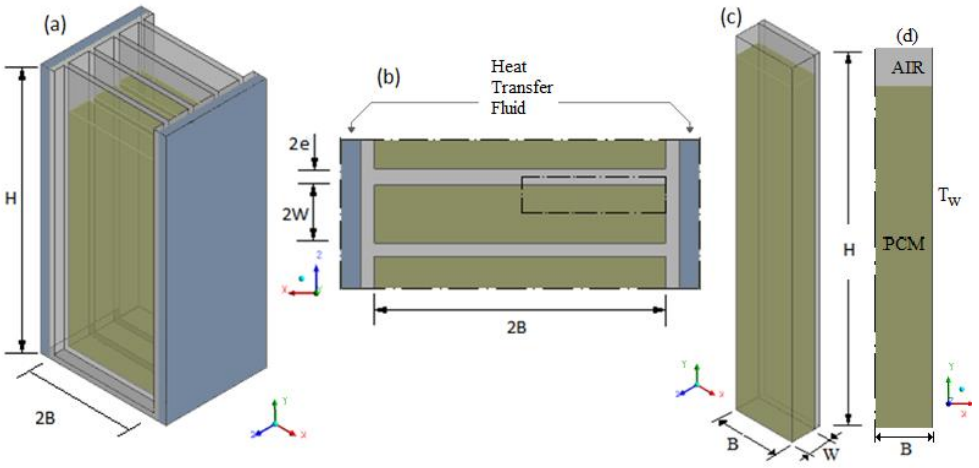

Figure 1. Geometry of the thermal energy storage system: (a) actual geometry; (b) view from top (within dashed line: 3D computational domain); (c) 3D computational domain and (d) 2D computational domain.

Table 1. Erythritol physical properties

Property	
Density (kg m^{-3})	1480(at 389 K); 1300 (at 413 K)
Latent heat capacity (J kg^{-1})	339800
Melting point (K)	391
Specific heat (J kg^{-1} K^{-1})	2250 (at 389 K); 2740 (at 413 K)
Thermal conductivity (W m^{-1} K^{-1})	0.733 (at 389K); 0.326 (at 413 K)
Viscosity (kg m^{-1} s^{-1})	0.000027749 T^2 - 0.0231747 T + 4.844
Thermal expansion coefficient (K^{-1})	0.00552825

2.2 Governing equations

The PCM liquid phase is assumed laminar due to the low velocity and small cavity size. The conservation equations, utilized in modeling PCM system in Cartesian coordinate system, through the enthalpy porosity approach, are (ANSYS-FLUENT, 2013):

$$\frac{\partial \rho}{\partial t} + \nabla.\left(\rho \vec{V}\right) = 0 \tag{1}$$

$$\frac{\partial \left(\rho \vec{V}\right)}{\partial t} + \nabla.\left(\rho \vec{V}\vec{V}\right) = -\nabla p + \nabla.\left(\mu \nabla \vec{V}\right) + \rho g + \vec{S} \tag{2}$$

$$\frac{\partial (\rho h)}{\partial t} + \nabla.\left(\rho \vec{V} h\right) = \nabla.(k \nabla T) \tag{3}$$

$$\frac{\partial (\alpha_n)}{\partial t} + \nabla.\left(\gamma_n \vec{V}\right) = 0 \tag{4}$$

where ρ is the density, t is the time, V is the velocity vector, p is the pressure, μ is the dynamic viscosity, S is the momentum source term, h is the enthalpy, k is the thermal conductivity, g is the gravity acceleration and T is the temperature. γ_n is the PCM's volume fraction on the umpteenth computational cell, assuming one of three conditions: if its value is 0, the cell does not contain PCM, if it is equal to 1, the cell is completely filled with PCM and if $0 < \gamma_n < 1$, the cell contains the interface between the PCM and one or more other fluids that exist in the computational domain, in this case, air.

The enthalpy is defined as a sum of the sensible enthalpy (hs) and the enthalpy change due to the phase change (γL), where h_{ref} is the reference enthalpy at the reference temperature T_{ref}, C_p is the specific heat, L is the specific

enthalpy of melting (latent heat of the material), and γ is the liquid fraction during the phase change which occurs over a range of temperature $T_s<T<T_l$, defined by the following relation (Shmueli *et al.* 2010):

$$h_s = h_{ref} + \int_{Tref}^{T} c_p \, dT, \tag{5}$$

$$\gamma = \begin{cases} 0 \text{ if } T < T_S, \\ 1 \text{ if } T > T_l, \\ \frac{T-T_s}{T_l-T_s} \text{ if } T_s < T < T_l. \end{cases} \tag{6}$$

The enthalpy-porosity technique considers the partially solidified region (mushy region) as a porous medium. The liquid fraction in each cell is considered the porosity in that cell. In fully solidified regions, the porosity is zero, which extinguishes the velocities in these regions. The momentum source term *S* in Eq. (2) takes the following form, due to the reduced porosity in the mushy zone (ANSYS-FLUENT):

$$\vec{S} = \frac{C\,(1-\gamma)^2}{(\gamma^3+\varepsilon)}(V - V_p) \tag{7}$$

where ε is a small constant (= 0.001) to avoid division by zero, C is the mushy zone constant and V_p is the solid velocity due to the pulling of solid phase out of the domain. Studied by some researchers [Voller and Prakash (1987), Brent *et al*. (1988), Shmueli *et al*. (2010), among others], C is a constant that depends of the morphology of the mushy zone (Voller and Prakash, 1987).

The simulations were conducted using the commercial software ANSYS-FLUENT (v14). The PRESTO scheme was used for the pressure correction, SIMPLE for the pressure-velocity coupling and QUICK to solve the momentum and energy equations.

2.3 Numerical Procedures

The numerical domain boundary conditions, post processing methods and numerical validations are presented in this section.

2.3.1 Boundary and initial conditions

The initial temperature of the air inside the cavity is equal to the initial temperature of the PCM (389 K). The numerical simulations were carried out for three temperature differences (ΔT) between T_w and the PCM melting temperature (T_m): 10, 15 and 20 ºC. All rigid walls were assumed as non-slipping. The bottom wall was assumed as adiabatic. A constant and uniform temperature was prescribed at the heating wall (T_w). The symmetry condition was used at all other walls. The coupled-wall boundary condition at the interface between PCM and fin is considered, to allow the conjugate heat transfer.

The computational domain consists of a cavity partially filled with PCM, while the rest is filled with air. This was done to allow the PCM volume expansion during heating. Thus, with the expansion of the PCM, a certain quantity of air must leave the cavity. At the cavity's top, the Pressure-Outlet condition was used, with Gauge Pressure=0 and Backflow Temperature=T_w. At the start of the simulation, the PCM occupies 85% of the cavity, while the air is used to fill the remaining 15%. The initial temperature of the whole domain is 2 °C below the PCM's melting temperature.

All spatial meshes are hexaedrical and constructed with the multi-block methodology and refinement near the solid walls and PCM-air interface. The mesh utilized was compared with two others, 30% and 50% more refined. No significant differences in melt fraction numbers was observed between the meshes, therefore, the original mesh was utilized.

2.3.2 Post Processing Method

Post processing was done through the ANSYS CFX-Post software. The remaining solid PCM volume for each time was obtained through mass fraction iso-surfaces, where the volume below the iso-surface is the solid PCM value. The melt fraction is then obtained using Eq. 8, presented as:

$$\gamma = 1 - \frac{V_{(t)}}{V_{(t=0)}} \tag{8}$$

Where γ is the PCM melt fraction (liquid fraction), $V_{(t)}$ is the solid PCM volume at a certain time and $V_{(t=0)}$ is the solid PCM volume at the start of the simulation. The melt fraction is a non-dimensional number that represents the volumes of liquid and solid PCM. If the melt fraction is equal to 1, all the PCM is in liquid state. Thus, if the melt fraction is equal to 0, all the PCM is solid.

2.4 Numerical Model Validation

The numerical validation was done using the results of Shmueli *et al.* (2010). The study consists of PCM melting in a vertical cylindrical tube. Two tube diameters (*D*) equal to 3 and 4 cm were used, with total height (H) of 20 cm. Only 17 cm were filled with PCM, to allow its expansion, while the remaining 3 cm were filled with air. The walls temperatures were either 10 or 30 °C above the PCM's melting temperature. The PCM used by Shmueli *et al.* (2010) was RT27.

The validation of the numerical model was presented in another paper by these same authors. A qualitative and quantitative melt fraction analysis was conducted. The results showed a good agreement between the results of Shmueli *et al.* (2010) and the results presented by the authors. The quantitative validation is presented in Fig. 2, which shows the comparison between the Melt fraction vs Time plots for the model utilized in this paper and the numerical and experimental results obtained by Shmueli *et al.* (2010). With these comparison, the model was considered as validated. (Raymundo Júnior, *et al.*, 2010).

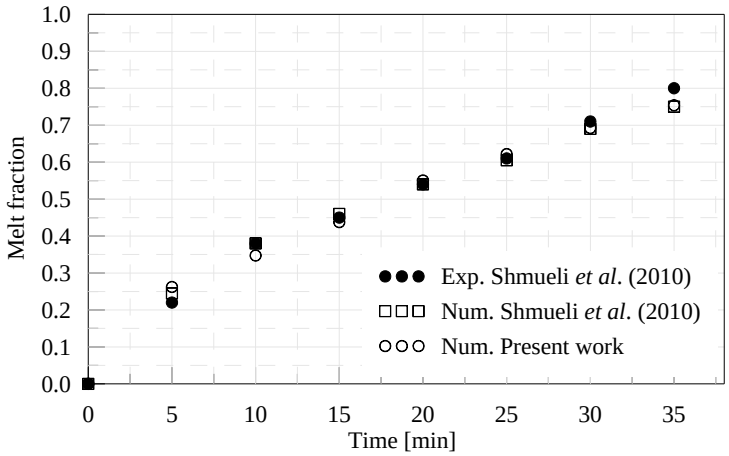

Figure 2. Melt Fraction vs Time, Experimental and numerical results of Shmueli *et al.* (2010) and model utilized in the present work.

3. NON-DIMENSIONAL NUMBERS

The thermal diffusivity of the solid phase (α), dimensional time (*t*) and *H* were used to define the Fourier number (*Fo*), as Eq. 9.

$$Fo = \frac{\alpha t}{H^2} \tag{9}$$

Others non-dimensional numbers must be used to achieve a valid correlation, which are: Stefan number (*Ste*) and Rayleigh number (*Ra*), as defined in Eqs. (10-11), respectively.

$$Ste = \frac{c_p \Delta T}{L} \tag{10}$$

$$Ra = \frac{g \beta \rho^2 c_p \Delta T H^3}{\mu k} \tag{11}$$

where β is the thermal expansion coefficient, ΔT is the temperature difference between the PCM's melting point and the wall temperature.

Several different cases with different geometries are taken into account. The cavity height (*H*), as well as its thickness (*W*) had three different values. The cavity height was either 10, 20 or 30 cm and its thickness was 2, 3 and 4 mm. These variations need to be taken into account when developing a correlation, so an aspect ratio (*AR*) is considered, defined as:

$$AR = \frac{H}{W} \tag{12}$$

4. RESULTS AND DISCUSSION

Figure 3 shows the melt fraction vs Fourier number plot for cases with W=4 mm and H=10, 20 and 30 cm for: (a) ΔT=10 °C, (b) ΔT=15 °C and (c) ΔT=20 °C. It is clearly noticeable that the value of H has a much bigger influence in the values of Fo than the temperature difference. This comes directly from the definition of Fourier number (Eq. 9), since doubling the temperature difference does not halves the melting time, but doubling the value of H reduces the Fourier number by four. It is also noted that, as the temperature difference between the PCM's melting point and the wall temperature increases (for the same H and W), the Fo, and thus, time, needed for a certain melt fraction to be achieved decreases. It is expected, since as you increase the ΔT the heat flux from the wall to the PCM drastically increases.

Table 2 shows a compilation of the values of Fourier number for all 27 cases. It shows the value of Fourier number when the melt fraction is 0.7 for every case. It is noted that the cases follow a pattern, increasing the value of Fo as you increase W and decreasing the Fourier number as H and ΔT increase. Also, there is a significant leap in the values of Fo as the value of H is increased. This behavior is explained due to the fact that H is chosen as the characteristic length of the studied problem. Thus, the value of Fo is highly dependent of H, since it is inversely proportional to H^2.

Table 2. Fourier number for γ= 0.7, H=10, 20, 30 cm, W=2, 3, 4 mm, ΔT =10, 15 e 20 ºC.

	Fo x 10^5								
	H=10 cm			H=20 cm			H=30 cm		
DT [ºC] / W [mm]	10	15	20	10	15	20	10	15	20
2	118.4	89.8	64.1	28.1	22.5	16.7	12.8	9.9	8.0
3	214.6	157.2	120.2	51.8	36.1	31.0	22.9	17.4	13.8
4	305.4	224.5	200.6	76.1	55.4	46.3	33.2	23.0	20.0

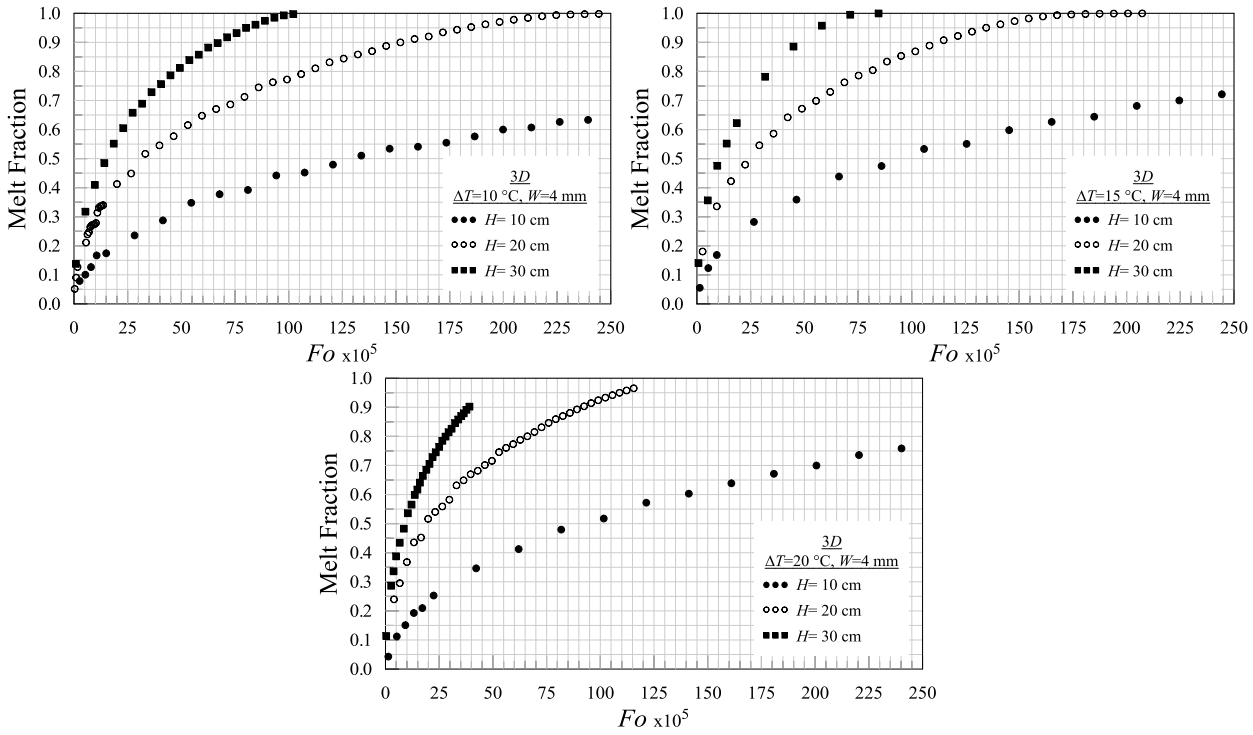

Figure 3. Melt Fraction vs. Fourier number for W=4mm and H=10, 20 and 30 cm for: (a) ΔT=10°C, (b) ΔT=15 °C and (c) ΔT=20°C.

With the results of 27 different cases, the melt fraction was calculated for various time values, through Eq. 9. This resulted in 2134 different entries. A non-linear regression was conducted through the DataFit software. This software

was chosen due to its great personalization capability on the model that is being utilized, allowing the user to create their own model, so that the software performs the non-linear regression to determine the coefficients for each variable. The non-linear regression resulted in the following correlation (Equation 13) between the melt fraction and the non-dimensional numbers presented previously. Each non-dimensional number has its own exponential coefficient and the whole equation is multiplied by another coefficient. All the achieved coefficients can be considered simple and easy to use.

$$\gamma = 0.55 Fo^{0.39} Ra^{0.08} Ste^{0.22} AR^{0.55} \tag{13}$$

The numerical correlation vs the correlation melt fraction plot is presented in Fig 2. It can be observed that the correlation shows good agreement with the numerical results. It is important to note that as the melt fraction value approaches 1, the deviation between the numerical results and the correlation results increases. The adjusted coefficient of multiple determination (Ra^2) for this correlation is equal to 0.9906, whereas a perfect fit would have a value equal to 1, which also indicates the good agreement between the numerical results and those obtained through the correlation.

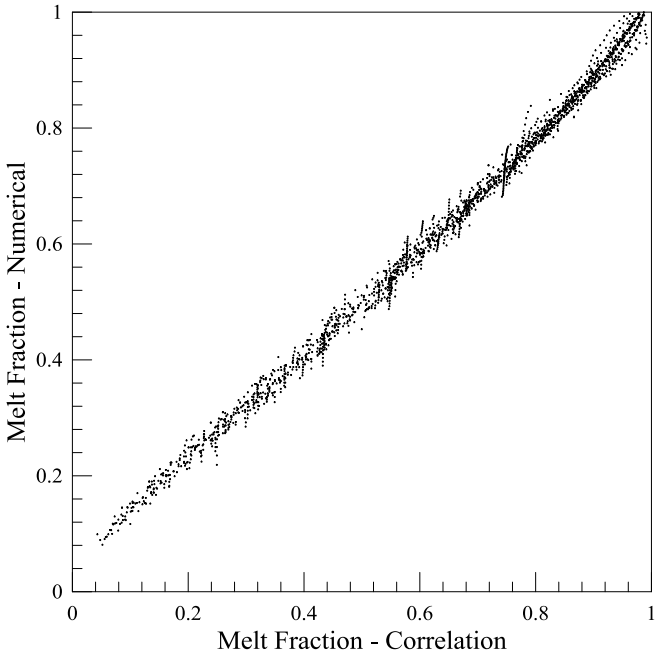

Figure 3. Numerical vs Correlation melt fraction plot

5. CONCLUSIONS

The aim of the present numerical study was to stablish a correlation between appropriate non-dimensional numbers and the PCM melt fraction during its melting process in a tall enclosure heat sink with inner fins. The PCM utilized in this study was Erythritol, due to its higher melting point compared to other PCMs largely studied in the literature. The study was conducted assuming different operational and geometric conditions. A constant temperature on one of the TES walls is considered. The 3D domain consisted of a tall enclosure heat sink with an inner fin. Three different values of ΔT, cavity height and spacing between the fins were considered. The numerical simulations were conducted through Computational Fluid Dynamics (CFD) with the Fluent (v14) software. The mathematical and numerical model utilized was validated through qualitative and quantitative comparison with results available in the literature, in terms of melt fraction vs time, displaying good agreement between the two. To stablish a melt fraction correlation, many relevant non-dimensional numbers are utilized. Fourier, Rayleigh and Stefan numbers are utilized, as well as an aspect ratio to link the geometric differences between the cases. Stefan and Rayleigh numbers are considered constant during the melting process. Melt fraction vs Fourier number plots are presented. It was concluded that the value of *Fo* is highly dependent on *H* and little by *W*. Also, that the higher the ΔT, lower the *Fo*, and thus, time, required for a certain melt fraction to be achieved, considering the same values of *H* and *W*. In other words, the higher the temperature difference, the faster the melting occurs. With a total of 27 different cases simulated and 2134 samples of melt fraction and time, a correlation was stablished. A non-linear regression was conducted through the DataFit software to achieve this correlation between the melt fraction and the non-dimensional numbers. A Numerical melt fraction vs the Correlation melt fraction plot is presented. It can be concluded that the presented correlation is highly capable of demonstrating the melt fraction behavior during the PCM melting process. The adjusted coefficient of multiple determination (Ra^2) is

0.9906, which confirms the good agreement between the numerical results and those obtained through the correlation. In this way, it can be concluded that the correlation proposed in this study is suitable for use when dimensioning similar tall enclosure heat sink based on PCMs.

6. REFERENCES

Agyenim, F., Eames, P., Smyth, M., 2010. "Heat transfer enhancement in medium temperature thermal energy storage system using a multitube heat transfer array". Renewable Energy, Vol. 35, No. 1, pp. 198-207.

Al-Abidi; Abduljalil A.; Mat, S.; Sopian, K.; Sulaiman, M.Y.; Mohammad, A. Numerical study of PCM solidification in a triplex tube heat exchanger with internal and external fins. Int. Journal of Heat and Mass Transfer, 61 (2013) 684-695.

ANSYS FLUENT. Release 14.0. Solver modeling Guide.

Assis, E.; Katsman, L.; Ziskind, G.; Letan, R., 2007 "Numerical and experimental study of melting in a spherical shell". Int. Journal of Heat and Mass Transfer, Vol 50, No. 9-10, pp. 1790-1804,.

Barba, A., Spiga, M. 2003. "Discharge mode for encapsulated PCMs in storage tanks." Solar Energy, Vol. 74, No. 2, pp. 141-148.

Brent, A. D., Voller, V. R., Reid, K. J. 1988. "Enthalpy-porosity technique for modeling convection-diffusion phase change: Application to the melting of a pure metal". Numerical Heat Transfer Vol. 13, No. 3, pp. 297-318.

Hesaraki, A. "CFD Modeling of Heat Charging Process in a Direct-contact Container for Mobilized Thermal Energy Storage". Disponível em http://www.diva-portal.org/smash/get/diva2:430712/FULLTEXT02. Acessed in 26/06/2015.

Rathod, M. K.; Benerjee, J. R., 2013. "Thermal stability of phase change materials used in latent heat energy storage systems: A review". Renewable and Sustainable Energy Reviews, Vol. 18, pp. 246-258.

Raymundo Júnior, J. F.; Borahel, R. S.; Oliveski, R. C. Numerical Simulation of the Erythritol Melting Process. In: 15th Brazilian Congress of Thermal Sciences and Engineering - ENCIT, 2014, Belém. 15th Brazilian Congress of Thermal Sciences and Engineering - ENCIT, 2014.

Saha, S. K.; Dutta, P., 2010."Heat transfer correlations for PCM-based heat sinks with plate fins". Applied Thermal Engineering, Vol. 30, No. 16, pp. 2485-2491.

Shatikian, V., Ziskind, G., Letan, R., 2005. "Numerical investigation of a PCM-based heat sink with internal fins: Constant heat flux". International Journal of Heat and Mass Transfer, Vol. 51, No. 5-6, pp. 1488-1493.

Shmueli, H., Ziskind, G., Letan, R., 2010. "Melting in a vertical cylindrical tube: Numerical investigation and comparison with experiments". International Journal of Heat and Mass Transfer, Vol. 53, No. 19-20, pp. 4082-4091.

Sillick, M., Gregson, C. M., 2012. "Spray chill encapsulation of flavors within anhydrous erythritol crystals". LWT-Food Science and Technology, Vol. 48, No. 1, pp. 107-113.

Voller, V.R., Prakash, C., 1987. "A fixed grid numerical modeling methodology for convection-diffusion mushy region phase-change problems". International Journal of Heat and Mass Transfer,Vol. 30, No. 08, pp. 1709-1719.

7. ACKNOWLEDGEMENTS

This work was financially supported by UNISINOS (University of Vale do Rio dos Sinos - Brazil), CAPES (Coordenação de Aperfeiçoamento de Pessoal de Nível Superior – Brazil) for the research project BEX 2614/13-8 and FAPERGS (Fundação de Amparo à Pesquisa do Estado do Rio Grande Sul).

8. RESPONSIBILITY NOTICE

The authors are the only responsible for the printed material included in this paper.